Relative multiple ionization cross sections of neon by projectiles in the 1–2-MeV/amu energy range*

Robert L. Kauffman,† C. W. Woods, K. A. Jamison, and Patrick Richard
Department of Physics, Kansas State University, Manhattan, Kansas 66506
(Received 11 November 1974)

The change in the $K\alpha$ x-ray spectra of neon is studied as a function of projectiles of $C^{+3,+4,+5,+6}$, $N^{+4,+6,+7}$, $O^{+4,+5,+6,+7,+8}$, and F^{+9} having an energy between 1 and 2 MeV/amu. The spectra are observed using a curved crystal spectrometer. Combined with previous measurements data are obtained for projectiles from carbon to argon. X rays are observed from different ionization states of Ne designated by KL^n for $n=1-7$. An 81% correction between the KL^5 peak and KL^6 peak is derived. Semiempirical fluorescence yields are applied to the relative x-ray intensities to obtain relative multiple ionization cross sections. These cross sections are fitted by a binomial distribution as predicted by Coulomb ionization. All cases give good fits except for the F^{+9} induced spectra. A possible explanation is that a different excitation mechanism may exist for this near-symmetric collision case.

I. INTRODUCTION

In recent studies of high-energy heavy-ion–atom collisions, data using gas targets have yielded surprising results. Winters *et al.*[1] and Mowat *et al.*[2] have observed an almost exponential increase in the x-ray production cross section of the gas targets as the charge state of the incident ion is varied. This is in contrast with Coulomb ionization theories which treat the projectile as structureless and predict no dependence on the ionic charge of the projectile.[3,4]

In a recent Letter it was reported that high-resolution techniques were used to resolve the K x rays emitted from a neon gas target bombarded by an oxygen projectile into a number of satellite lines corresponding to different amounts of multiple L-shell ionization.[5] In these spectra it is shown that the amount of L-shell ionization also depends upon the ionic charge of the projectile. In this paper a systematic study is done of the relative intensity of the K x-ray satellite structure of neon for various projectiles with different incident charge (C^{+3-+6}, $N^{+4,+6,+7}$, O^{+4-+8}, F^{+9}). Combined with other published data[6–8] this provides data of the satellite structure of neon for projectiles ranging from protons to argon in the 1–2-MeV/amu energy range.

After an ion-atom collision in which a K-shell vacancy is produced, the atom can de-excite by emitting an x ray or an Auger electron. To measure the total vacancy-production cross section, both the x-ray production cross section and Auger-electron production cross section should be measured. Auger-electron measurements for neon have proven to be difficult and relatively few measurements have been performed.[9] Another approach is to measure the x-ray-production cross section and apply a fluorescence-yield correction to obtain a vacancy-production cross section. Bhalla *et al.* have shown that the fluorescence yield is a function of the number of electrons present in the outer shell of the atom, or of the atom's charge state.[10] High-resolution measurements such as those presented in this paper combined with poor-resolution measurements can be used to obtain vacancy-production cross sections.[9]

The high-resolution measurements are also important because they contain information concerning the multiple ionization of the L shell. These can be used to test existing theories concerning multiple ionization.[11,12]

II. EXPERIMENT

The experiment is performed using beams of carbon, nitrogen, oxygen, and fluorine obtained from the Kansas State University tandem Van de Graaff accelerator. The beam is energy analyzed and passed through a thin (20-μg/cm^2) carbon stripper foil as shown in Fig. 1. The stripper foil also could be removed to allow the beam in its original charge state to be passed directly into the detection apparatus. The beam in the desired charge state is selected by the switching magnet and passed through a differentially pumped gas cell. The gas cell consists of four apertures dividing the cell into four regions: the first intermediate region, the target region, the second intermediate region, and the beam collection region. The set up has been varied but a representative set of apertures from front to rear consists of holes having 2-, 2-, 3-, and 4-mm diameters, respectively. Some of the data were taken without the fourth aperture without any noticeable change in the data. For 0.1 Torr of neon in the target region, the pressure in front of the gas cell, which is approximately 10 m from the switching magnet,

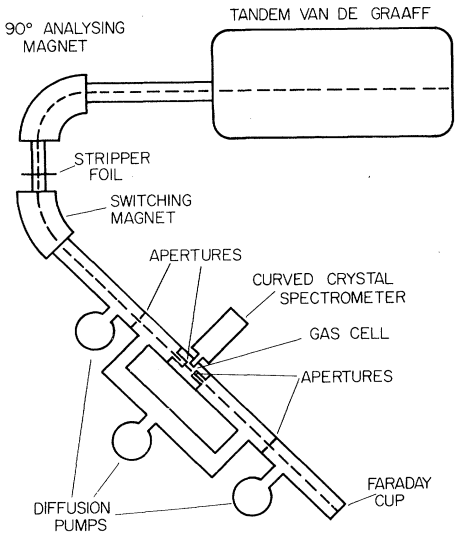

FIG. 1. Schematic of the experimental apparatus used in the experiment. The stripper foil between the magnets may be removed to allow the direct beam to pass through the gas cell. The curved crystal spectrometer is at 90° to the beam axis.

is 2×10^{-6} Torr. For the intermediate regions, each 30 cm in length, the pressure is 5×10^{-5} Torr. The beam is estimated to contain better than 98% of the pure charge state upon entering the target region.

A schematic of the target region is shown in Fig. 2. The beam passes in front of the 1.6-cm slit of the x-ray spectrometer which is perpendicular to the beam axis. The pressure in the cell is kept constant using a mechanical leak valve in conjunction with a capacitance manometer. A solid target may also be used for calibration purposes.

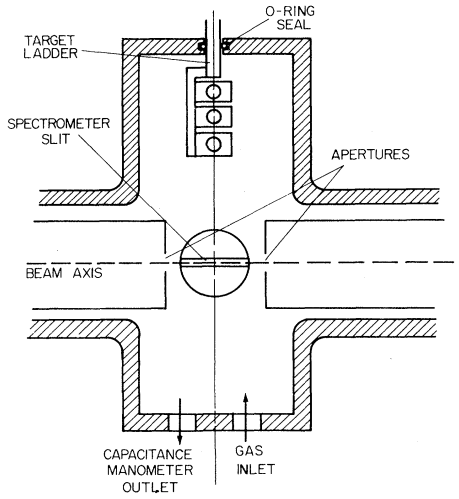

FIG. 2. Enlarged schematic of the detection region. Solid targets as well as gas targets may be used for calibration and alignment purposes.

The x rays are detected using a 4 in. curved crystal spectrometer.[13] A rubidium acid phthalate (RAP) crystal ($2d$ spacing = 26.121 Å) is used to diffract the x rays. A typical spectrum is shown in Fig. 3. The identification of the various peaks will be discussed below. A proportional counter having a 2-μm Macrofol window is used to detect the x rays.[14] The pulses from the proportional counter are amplified and pulse height analyzed using a single-channel analyzer. The energy acceptance window is set using L x rays of nickel and beam x rays of oxygen and fluorine. The pulses are collected in a PDP-15 computer for a specified amount of integrated beam current. The computer automatically moves the spectrometer in constant wavlength intervals thus generating the spectra as shown in Fig. 3. The lower spectrum shown in Fig. 3 was taken with the same apparatus as the upper spectrum only using a mica crystal ($2d$ spacing = 19.840 Å). The mica crystal gives better resolution than the RAP crystal. Despite the better resolution no new features are observed and the results as discussed below are essentially the same for the two spectra. The largest advantage in using the RAP crystal is that the counting rate is almost an order of magnitude greater than that for the mica crystal. This

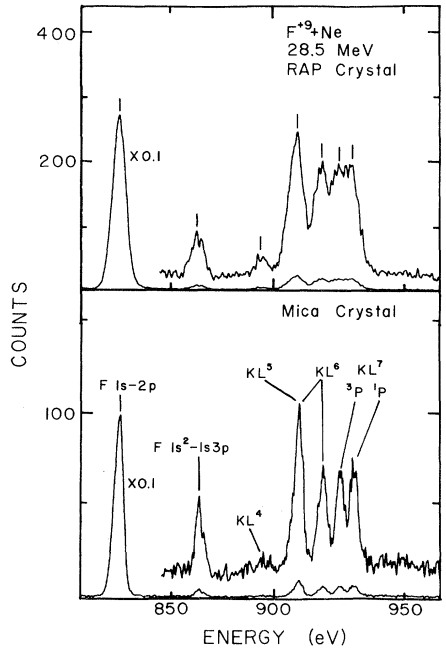

FIG. 3. X-ray spectra of F^{+9}+Ne at 28.5 MeV. The top spectrum has been taken using a RAP crystal. In the bottom spectrum a mica crystal is used. The difference in resolution is due to the difference in $2d$ spacings. The RAP crystal gave almost an order-of-magnitude better yield. The low-energy peaks are due to the fluorine beam.

aids in obtaining useful results for some charge state even when only small beam currents are available.

III. RESULTS

Spectra produced by bombardment of neon by O^{+4} and O^{+8} at 24 MeV are shown in Fig. 4. The peaks in Figs. 3 and 4 are labeled according to the convention of Ref. 5 where K^mL^n denotes the peak having m K-shell vacancies and n L-shell vacancies. Some high-energy peaks in the O^{+8} spectrum which do not conveniently fit this notation are labeled according to the electronic configuration of the transition. The ^1P and ^3P He-like KL^7 peaks of Ne are better resolved in Fig. 4 than in Fig. 3. This results from the use of a smaller exit slit collimator in front of the proportional counter for the data given in Fig. 4. Hydrogenlike and heliumlike fluorine peaks are seen in Fig. 3 and hydrogenlike oxygen peaks are observed in Fig. 4. The measured energies of the neon peaks are given in Table I. These are a composite of all of the measurements performed in this paper. The spectra are calibrated using the hydrogenlike lines of oxygen and fluorine after correction for the transverse Doppler shift.[15] Also given are measurements by Matthews *et al.*[6] from oxygen-induced neon spectra and measurements by Peacock *et al.*[16] using a plasma source. Also shown are Hartree-Fock-Slater calculations by Bhalla *et al.*[10] for the initial hole configurations of $(1s)^m(2s)^q(2p)^r$,

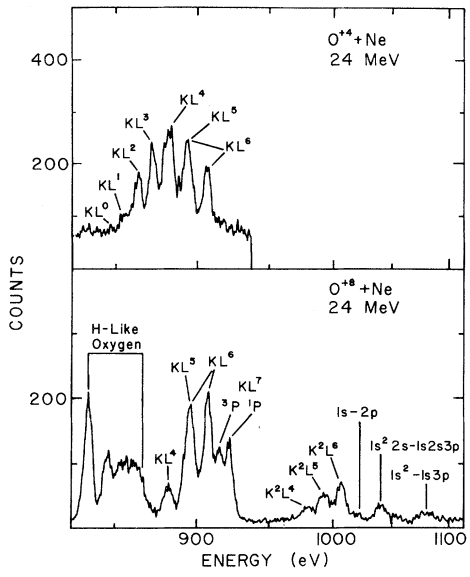

FIG. 4. Spectra produced by 24-MeV O^{+4} and O^{+8} on Ne. The low-energy structure in the bottom spectrum is from the oxygen beam. The assignments of the neon peaks are discussed in the text.

TABLE I. Energies (in eV) of the various observed neon peaks.

	Present	Others a	Others b	Initial configuration $(1s^m2s^q2p^r)$ m	q	r	Calculated[c]
KL^0	848.5	848.6		1	2	6	848.5
KL^1	855.0	854.8		1	2	5	853.7
				1	1	6	854.6
				1	2	4	860.7
KL^2	863.6	862.1		1	1	5	860.9
				1	0	6	861.7
				1	2	3	869.0
KL^3	872.4	871.1		1	1	4	868.9
				1	0	5	869.2
				1	2	2	879.0
KL^4	882.5	880.4		1	1	3	878.5
				1	0	4	878.3
				1	2	1	890.7
KL^5	896.5	894.3		1	1	2	889.7
				1	0	3	889.0
KL^6	908.4	906.0	904.2	1	2	1	902.6
			908.1	1	0	2	901.6
KL^7 ^3P	915.9	914.0	914.8				
^1P	922.5	920.8	922.0	1	0	1	914.4
				0	2	2	982.3
K^2L^4	979.6			0	1	3	980.9
				0	0	4	979.9
				0	2	1	995.3
K^2L^5	992.9			0	1	2	993.5
				0	0	3	992.0
K^2L^6	1006.8		1003.4	0	1	1	1007.6
			1007.6	0	0	2	1012.5
$(1s2s3p)-(1s^22s)$	1040.5		1041.4				
$(1s3p)-(1s^2)$	1083.3		1073.9				

[a] From Ref. 6.
[b] From Ref. 16.
[c] From Ref. 10.

where $q+r=n$. Except for the normal KL^0 line, the present measurements are seen to be consistently higher than the values of Matthews *et al.* The present values also agree with the lines measured by Peacock *et al.*[16] and they agree somewhat with the calculations of Bhalla *et al.*[10] These indicate that the assignments are correct.

The relative intensities of the Ne $K\alpha$ satellite structure, $R_{KL}n$, are given in Table II. These values are obtained by fitting spectra such as those in Figs. 3 and 4 to a number of Gaussian peaks. The results are corrected for crystal reflectivity[17] and quantum efficiency of the detector[14] using the values given in Table II. Most of the data are taken at the ion velocity of 1.5

TABLE II. Relative x-ray-production cross sections, R_{KL^n}, for C^{+3-+6}, $N^{+4,+6,+7}$, O^{+4-+8}, and F^{+9}.

Beam type	Energy (MeV)	Pressure (Torr)	R_{KL^0}	R_{KL^1}	R_{KL^2}	R_{KL^3}	R_{KL^4}	R_{KL^5}	R_{KL^6}	R_{KL^7}
C^{+3}	18	0.13	0.031(8)	0.125(9)	0.240(25)	0.237(25)	0.205(25)	0.123(19)	0.040(7)	
C^{+4}	18	0.15		0.090(55)	0.187(32)	0.277(37)	0.219(35)	0.160(28)	0.068(17)	
C^{+5}	18	0.20		0.074(9)	0.164(28)	0.235(36)	0.238(33)	0.201(28)	0.088(9)	
C^{+6}	18	0.10		0.043(19)	0.095(20)	0.119(20)	0.245(24)	0.254(23)	0.155(20)	0.087(16)
N^{+4}	21	0.10		0.048(14)	0.156(23)	0.248(28)	0.233(27)	0.180(22)	0.086(17)	0.048(12)
N^{+6}	21	0.10			0.076(10)	0.167(19)	0.259(22)	0.314(21)	0.148(15)	0.037(9)
N^{+7}	21	0.10			0.026(10)	0.062(17)	0.173(24)	0.358(27)	0.229(25)	0.151(29)
N^{+7}	25.5	0.20		0.024(8)	0.065(9)	0.128(9)	0.186(9)	0.273(9)	0.218(8)	0.106(5)
O^{+4}	24	0.10		0.031(8)	0.128(13)	0.163(15)	0.324(21)	0.224(14)	0.129(10)	
O^{+5}	24	0.10			0.102(11)	0.203(36)	0.281(38)	0.285(52)	0.130(23)	
O^{+5}	30	0.10		0.061(10)	0.138(32)	0.159(28)	0.229(30)	0.223(24)	0.132(19)	0.058(7)
O^{+6}	24	0.10			0.079(16)	0.151(24)	0.242(30)	0.293(29)	0.174(22)	0.060(11)
O^{+6} [a]	35	0.05	0.014	0.054	0.135	0.205	0.237	0.221	0.102	0.033
O^{+7}	24	0.10				0.090(10)	0.203(12)	0.346(16)	0.255(14)	0.107(16)
O^{+7}	30	0.10		0.027(4)	0.077(4)	0.105(12)	0.210(15)	0.287(13)	0.210(15)	0.075(10)
O^{+7} [a]	35	0.05		0.033	0.098	0.183	0.243	0.272	0.137	0.034
O^{+8}	24	0.10					0.104(11)	0.344(17)	0.291(20)	0.261(31)
O^{+8}	30	0.10					0.139(14)	0.390(17)	0.268(18)	0.202(10)
O^{+8} [a]	35	0.05			0.031	0.074	0.172	0.331	0.249	0.142
F^{+9}	28.5	0.075					0.034(6)	0.347(16)	0.222(25)	0.397(67)
F^{+9}	35.6	0.075					0.041(13)	0.419(16)	0.285(16)	0.254(29)
Cl^{+7} [b]	40	0.050					0.086(8)	0.379(32)	0.331(32)	0.204(27)
Cl^{+11} [b]	40	0.050						0.336(33)	0.314(35)	0.351(62)
Cl^{+13} [b]	40	0.050						0.280(20)	0.236(22)	0.484(32)
Ar^{+6} [c]	80	0.20				0.058(9)	0.214(17)	0.321(14)	0.223(11)	0.184(18)
Ar^{+14} [c]	80	0.20					0.044(5)	0.286(22)	0.249(26)	0.421(18)
Reflectivity $\times 10^5$ [d]			7.8	7.9	8.0	8.1	8.2	8.3	8.4	8.5
Quantum efficiency [e]			0.37	0.38	0.39	0.40	0.41	0.42	0.43	0.44

[a] From Ref. 6.
[b] From Ref. 7.
[c] From Ref. 8.
[d] From Ref. 17.
[e] From Ref. 14.

MeV/amu. Here data are obtained for $C^{+3,+4,+5,+6}$, for $N^{+4,+6,+7}$, for $O^{+4,+5,+6,+7,+8}$, and for F^{+9}. The N^{+5} beam is too weak to obtain any results. Only the F^{+9} case could be measured in the fluorine case because the neon $K\alpha$ lines have approximately the same energy as the fluorine heliumlike transitions. In the F^{+9} case the projectile must acquire two electrons to reach a heliumlike state. This can be done by double collisions in which the projectile captures an electron in each collision. By adjusting the gas pressure the probability for this process can be made negligibly small. The heliumlike system can be formed from the bare nuclei by a double-electron capture during a single collision. This process is much less likely than a single-electron capture.[18] This is the process that gives the small heliumlike $(1s)^2$-$(1s)(3p)$ transition observed in Fig. 3. The other heliumlike fluorine lines which lie under the neon lines have been shown to have almost negligible intensity when argon is used as the target gas.[19] These give negligible contributions to the neon intensities. Data are also obtained at about 1.87 MeV/amu N^{+7}, $O^{+5,+7,+8}$, and F^{+9}. Combined with the measurements of Matthews *et al.*,[6] the general trend of the oxygen satellite structure as a function of energy can be seen. Also included in Table II are previously published measurements for chlorine and argon projectiles,[7,8] giving data on the neon satellite structure over a large range of projectiles.

The intensities of the high-energy lines above the $K\alpha$ satellite group have not been measured. For the cases studied here the intensity of these lines is negligible compared with the satellite intensity. In most cases the higher energy lines are not discernible. For chlorine, where these lines are readily observed, their contribution to the vacancy production cross section is small.[7] For the lower Z projectiles these contributions would be even smaller.

In the discussion concerning the peak assign-

ments, the use of K^mL^n notation oversimplifies the process. In the data the heliumlike transitions $(1s2p)\,^3P$-$(1s^2)\,^1S$ and $(1s2p)\,^1P$-$(1s^2)\,^1S$ are partially resolved. The difference in energy between these two transitions is due to the term splitting between the ^1P and ^3P level. This energy difference is on the order of the splitting between peaks assigned to a certain electronic configuration. The term splittings between all levels should be calculated to test the assumption that each peak corresponds to a single charge state as implied by the K^mL^n notation. Preliminary calculations using a single-configuration Hartree-Fock approximation have been made.[20] These indicate that there may be a small overlap between different charge states but that the majority of the lines group about the centroid of the observed peak.[21] Because for most of the charge states there is a large number of lines and most of these are grouped closely around the centroid, little accuracy should be lost in treating each peak as belonging to a specific charge state.

IV. THREE-ELECTRON SYSTEM

The decay of the three-electron system needs to be studied more closely. Beam-foil studies have shown that the $(1s2s2p)\,^4P$ and $(1s2p^2)\,^4P$ have radiative decays to the $(1s^22s)\,^2S$ and $(1s^22p)$-^2P states for atoms around the Z of neon.[22,23] The energy difference between these normally forbidden decays and the decay of the doublet levels is as large as the energy difference between satellite groups. The calculated energies of the transitions of the three-electron system for neon are given in Table III. The second column gives the energies obtained by using a single-configuration Hartree-Fock calculation.[24] The third column gives the results of a Z-expansion calculation.[25] Comparing these values with the values in Table I, it is seen that the transitions between doublet levels correspond to the calculations of Bhalla *et al.*[10] for the three-electron system and to the observed value of the peak KL^6. The quartet decays have approximately the same energy as the KL^5 peak. To obtain relative ionization cross sections the data must be corrected for this effect.

TABLE III. Calculated transition energies for the three-electron system of neon.

Transition	Energy (eV) Hartree-Fock[a]	Z expansion[b]
$(1s2s2p)$-$(1s^22s)$		
^4P-^2S	894.2	895.4
$(^3P)\,^2P$-^2S	898.9	914.6
$(^1P)\,^2P$-^2S	913.1	907.4
$(1s2p^2)$-$(1s^22p)$		
^4P-^2P	895.2	897.0
^2D-^2P	903.7	805.8
^2P-^2P	905.3	908.2
^2S-^2P	911.0	917.1

[a] See Ref. 24.
[b] See Ref. 25.

The decay scheme for the three-electron system of neon is shown in Fig. 5. The energy levels are those given by the single-configuration Hartree-Fock calculations.[24] The decay of the fully allowed doublet transitions are indicated by the solid lines. The decay of $(1s2s2p)\,^4P_{1/2,3/2}$ and $(1s2p^2)\,^4P_{1/2,3/2}$ states to the $(1s^22s)\,^2S$ and $(1s^22p)\,^2P$ states are indicated by dashed lines. These normally forbidden transitions occur by mixing with the $(1s2s2p)\,^2P_{1/2,3/2}$ and $(1s2p^2)\,^2P_{1/2,3/2}$ states as indicated by the wavy lines.[26] The $J=\frac{5}{2}$ components of the ^4P states do not couple with the doublet states and do not have a radiative branch to the doublet states.[27]

To correct the data for the overlap of R_{KL^6} with R_{KL^5}, the ratio of the number of radiative decays from the quartet states N_4 to the number of radiative decays from the doublet states N_2 needs to be known. The number of radiative decays from a given multiplicity N_S can be estimated by using the formula

$$N_S = \sum_{\alpha} n(\alpha) \sum_{L,J} g(\alpha, L, \boldsymbol{J})\omega(\alpha, L, J), \qquad (1)$$

where the sum over α is a sum over all possible initial configurations in the three-electron system

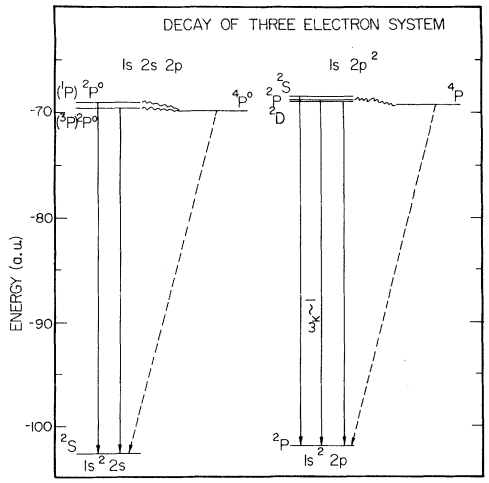

FIG. 5. The decay of the three-electron system of neon. The energies are from Ref. 24. The allowed decays are designated by the solid lines. The forbidden decays are designated by the dashed lines. The wavy lines indicate the coupling between states.

and the sum over L and J ranges over all possible states having the given multiplicity S. $n(\alpha)$ is the initial population of the configuration α. In this analysis it is assumed that the different configurations are populated randomly and that the probability for creating a $2s$ and $2p$ hole are equal. Thus the configurations $1s2p^2$, $1s2s2p$, and $1s2s^2$ are assumed to be populated in a ratio of 15:12:1.

$g(\alpha, L, \boldsymbol{J})$ is the relative initial population of a given state labeled by S, L, and $\boldsymbol{J}$ in the configuration α. For a statistical population each state is weighted by $(2J+1)$ so that $g(\alpha, L, J) = (2J+1)/\sum_j (2J+1)$, where the sum is over all states in the given configuration. For $1s2p^2$ configuration there are 30 components so that $g = (2J+1)/30$ for that configuration. In the $1s2s2p$ configuration there are 24 possible components and $g = (2J+1)/24$. For the $1s2s^2$ configuration the only possible state is $^2S_{1/2}$, so that $g = 1$ is that case.

In Eq. (1), $\omega(\alpha, L, J)$ is the fluorescence yield for that particular state, or the x-ray branching ratio for that state. Bhalla *et al.*[10] have calculated these numbers using wave functions for the average state in each configuration. No multiplet effects are considered. Bhalla has recently performed calculations for doubly ionized neon including the multiplet effects and has shown that the fluorescence yield depends on the multiplet level considered.[28] The dependence is due to the change in the wave functions by the electron-electron interactions. Since calculations have not been made for the three-electron system, each multiplet level is assumed to decay with the same fluorescence yield as the average configuration except when selection rules close one of the possible decay channels. The $(1s2p^2)^2P$ and ^2S levels are assumed to have a fluorescence yield of 0.0823.[10] The $(1s2s2p)^2P$ and $^4P_{1/2,3/2}$ levels are assumed to have $\omega = 0.0843$. The decay of the $1s2s^2$ configuration to the ground state is not observed in this experiment so that $\omega = 0$. The $(1s2p^2)^2P$ has its Auger channel closed under the dipole approximation. The selection rules are that $\Delta L = 0$, $\Delta S = 0$, $\Delta J = 0$, and no change in parity.[29] For the $(1s2p^2)^2P$ state to undergo Auger decay to the $(1s^2)^1S$ state, a p-wave electron must be emitted to satisfy $\Delta L = 0$. The $^1S + p$-wave state has odd parity because a p-wave electron has odd parity. This transition violates the parity conservation rule because $(1s2p^2)^2P$ has even parity. Thus, the fluorescence yield for the $(1s2p^2)^2P$ state is one. Since the $(1s2p^2)^4P_{1/2,3/2}$ state decays primarily as a result of coupling with the ^2P state, the fluorescence yield for the $^4P_{1/2,3/2}$ state is also one. The Auger channel may not be completely closed because some configuration mixing may occur. This would make the fluorescence yield not exactly but almost one. The $^4P_{5/2}$ states have a fluorescence yield of zero since there is no x-ray branch.

Substituting the above values into Eq. (1), the ratio of the number of quartet x-ray decays to the number of doublet x-ray decays, N_4/N_2, is found to be 0.81. Thus to find the true amount of R_{KL^5} and R_{KL^6}, 81% of the R_{KL^6} intensity must be subtracted from R_{KL^5} and added to R_{KL^6}. The value of N_4/N_2 depends upon the assumption of a statistical initial population, upon the fluorescence yields used, and upon the assumption of strong coupling between the quartet and doublet states.

V. FLUORESCENCE YIELDS

The fluorescence yield for a particular state $\omega(\alpha, L, J)$, as referred to earlier, can be defined as

$$\omega(\alpha, L, \boldsymbol{J}) = \frac{\Gamma_x}{\sum_i \Gamma_i} \quad , \tag{2}$$

where the numerator is the x-ray decay rate and the denominator is the sum of the decay rates of the competing transition from that state. This differs from the usual definition,[10] $\omega_K = \Gamma_x/(\Gamma_x + \Gamma_A)$, only by the inclusion of all possible decay modes of the state. This becomes important only in the few-electron systems. Eq. (2) explicitly accounts for other possible decay modes such as two-photon emission. It should be noted that for systems which include large amounts of one- and two-electron systems that the average fluorescence yields[9] $\bar{\omega} \neq \sigma_x/(\sigma_x + \sigma_A)$ since this would not include all of two-photon decays and metastable decays which are not detected.[30]

The observed x-ray groups are from states having a specific degree of ionization and not from specific L, S, J states. $\omega(\alpha, L, J)$ must be averaged over the initial populations of each state to obtain a fluorescence yield ω_{KL^n} for a particular ionization state KL^n. This requires that an initial population must be assumed. A complete set of calculations for $\omega(\alpha, L, \boldsymbol{J})$ have not been performed. Bhalla has calculated $\omega(\alpha, L, \boldsymbol{J})$ for the $(1s2s^22p^5)^3P$ and ^1P states and obtains values of 0.013 and 0.028, respectively.[28] Using a statistical population of ^3P: ^1P of 9:3, $\omega(1s2s^22p^5) = 0.0167$ which is in agreement with the previous calculations.[10] Bhalla *et al.*[31] have given evidence that the states may not be statistically populated but that the population is approximately the same for a variety of projectiles. The nonstatistical population would affect the correction to the three-electron peak as discussed previously and would affect the fluorescence yields derived by Bhalla *et al.*[10] If the states are populated the same way, independent of projectile, a set of fluorescence yields may be derived which

can be used for all sets of data.

A set of semiempirical fluorescence yields are given in Table IV derived by Stolterfoht *et al.*[32] These values are obtained by using high-resolution x-ray intensities such as those given in Table I, high-resolution Auger intensity ratios for KL^0 and KL^1,[33] and the ratio of x-ray to Auger production cross section.[9] A binomial distribution for relative intensities is assumed. For comparison the calculated fluorescence yields of Bhalla *et al.*[10] are also given in Table IV. These are derived assuming a statistical population among the different configurations. The difference between the two sets of values is greater for the larger amounts of multiple ionization. The largest difference is for KL^6 where the calculations do not take into account the closed Auger channel of the $(1s2p^2)^2P$ and ^4P states.

The value of ω_{KL^7} of 0.375 given in Table IV is derived assuming that no long-lived metastable decays are observed. The fluorescence yield is not one even though no Auger processes can occur because the $(1s2p)^3P_{0,2}$ cascade to the $(1s2s)^3S_1$, which in turn decays by a magnetic dipole transition to the $(1s^2)^1S_0$ state. The $(1s2p)^3P_2$ can also decay to the $(1s^2)^1S_0$ state via a magnetic quadrupole transition.[31] The mean lifetime for the $^3P_2$-$^1S_0$ and $^3S_1$-$^1S_0$ decays are 448 (Ref. 34) and 92 000 nsec,[35] respectively. These states are not observed in this experiment due to recoiling from the detection region before decay. The $^3P_1$-$^1S_0$ decay which proceeds by mixing with the $^1P_1$ state has a mean lifetime of 0.18 nsec,[36] and its decay should be totally observed. Table V shows the measurements of the ratio $^1P/^3P$ for different projectiles. Matthews *et al.*[6] quote a value of 1.6 but the measurements of this paper and other works[7] give a value closer to 1.1 which is near the theoretical value of one given assuming statistical population and total detection. The agreement gives some confidence to both assumptions.

TABLE IV. Neon K-shell fluorescence yield ω_{KL^n} for the ionization state KL^n.

n	ω_{KL^n} Semi empirical[a]	ω_{KL^n} Calculated[b]
0	0.016	0.0160
1	0.018	0.0174
2	0.021	0.0195
3	0.022	0.0229
4	0.045	0.0289
5	0.051	0.0416
6	0.378	0.0802
7	(0.375)	...

[a] From Ref. 32.

[b] From Ref. 10. These values are obtained by assuming a statistical population of the different configurations.

TABLE V. Measured values of the ratio $^1P/^3P$ in the two-electron system of neon.

Projectile (energy)	$^1P/^3P$
O^{+8} (35 MeV)[a]	1.6
F^{+9} (28.5 MeV)	1.13
Cl^{+7} (40 MeV)[b]	1.08
Cl^{+11} (40 MeV)[b]	1.04
Cl^{+13} (40 MeV)[b]	1.14

[a] From Ref. 6.

[b] From Ref. 7.

The theoretical fluorescence yields as calculated by Bhalla (last column in Table IV) are obtained by taking the *average* total x-ray rate, $\bar{\Gamma}_x$, and Auger rates, $\bar{\Gamma}_A$, for various electronic configurations. These rates were obtained by taking an average over the spectroscopic terms assuming a statistical population. Bhalla[37] and Chen and Craseman[38] have recently pointed out that significantly different fluorescence yields are obtained by calculating by the weighted average of the fluorescence yields of the individual multiplet states in the spirit of Eq. (1). We therefore expect that the discrepancies will be removed with properly calculated fluorescence yields.

VI. THEORY

Several theories of vacancy production have been developed for heavy-ion–atom collisions.[39] The molecular-orbital theory has been successful in describing vacancy production in low-energy collisions.[40] Here the electrons are assumed to adjust adiabatically in molecular orbitals during the collision. At intermediate energies the concept of diabatic orbitals can be used to qualitatively explain the data.[41] To use these concepts the average electron velocity, $v_e = (2U/m)^{1/2}$, where U is the electron binding energy and m is the electron mass, must be greater than the incident projectile velocity v_i, or $V = v_i/v_e < 1$.[39] For the collisions considered here $V_L > 1$. In these collisions the scaled velocity of the K shell, V_K is approximately one. Some molecular effects may be observed in the K-shell cross section even though the L-shell cross section would have no such effects. The use of molecular orbitals has been extended to higher energy for near symmetric collisions[42] but multiple ionization has not been considered.

Several ionization theories treating the impinging projectile as a structureless particle have been developed. The semiclassical approximation[11] (SCA) and the binary-encounter approximation[12] (BEA) have the same starting point for multiple ionization. The cross section $\sigma_{K^mL^n}$ for ioniza-

tion of m K-shell electrons and n L-shell electrons is given by

$$\sigma_{K^m L^n} = \int 2\pi b\, db \binom{2}{m} P_K^m(b) \times [1 - P_K(b)]^{2-m} \binom{8}{n} P_L^n(b)[1 - P_L(b)]^{8-n}, \tag{3}$$

where $P_K(b)$ and $P_L(b)$ are the probability per electron for ionization of the K and L shells, respectively, and $\binom{x}{y}$ are binomial coefficients. $P_K(b)$ and $P_L(b)$ are written explicitly as functions of the impact parameter b. In the above expression the probability for ionization of the $2s$ and $2p$ subshells are considered to be equal. If $P_K(b) \ll 1$, the expression becomes for single K-shell ionization

$$\sigma_{KL^n} = \int 2\pi b\, db\, 2P_K(b) \binom{8}{n} P_L^n(b)[1 - P_L(b)]^{8-n}. \tag{4}$$

The two theories differ in their methods of calculating $P_K(b)$ and $P_L(b)$. The SCA theory treats the projectile as having a classical trajectory and uses perturbation techniques to compute the probability for ionization of the target by the projectile following that trajectory.[43] The BEA theory uses the expression for cross section for ionization and transforms this expression into one containing an impact parameter. By comparison of this expression with $\sigma = \int 2\pi b P(b)\, db$, an expression for $P(b)$ can be obtained.[12] For both treatments, in the region where $P_K(b)$ is nonzero $P_L(b)$ is almost constant so that $P_L(b)$ can be replaced by the probability for L-shell ionization at zero-impact parameter, $P_L(0)$. Equation (4) reduces to

$$\sigma_{KL^n} = \binom{8}{n} P_L^n(0)[1 - P_L(0)]^{8-n} \sigma_K, \tag{5}$$

in agreement with Eq. (34) of Ref. 12. Thus the multiple ionization should follow roughly a binomial distribution. This has been demonstrated for solid targets[44] but has not been proven for gas targets.

$P_L(0)$ has been given in the BEA theory as[12]

$$P(0) \cong \frac{\sigma(E)/N}{\pi R^2}, \tag{6}$$

where R is given by $R \cong \sqrt{2}\, A$; A is the mean radius of the electron orbital. $\sigma(E)/N$ is the cross section for ionization per electron given by

$$\frac{\sigma(E_i)}{N} = \frac{Z^2 \sigma_0}{U^2} G(V). \tag{7}$$

Z is the projectile charge and $\sigma_0 = 6.56 \times 10^{-14}$ cm^2 eV^2. U is the electron binding energy and $G(V)$ is a function of the scaled velocity whose value is tabulated in Ref. 12. No simple formulas have been developed in the SCA theory, but it does predict the same Z^2 scaling with projectile charge.[43] Calculations in the SCA theory for $P_L(b)$ have not been performed in the scaled velocity range of this experiment.

VII. DISCUSSION

Relative ionization cross sections can be obtained from the relative x-ray intensities given in Table I by using the formula $\sigma_{KL^n} = R_{KL^n}/\omega_{KL^n}$ combined with the semiempirical fluorescence yields given in Table IV. The relative ionization cross sections are given in Table VI. The values have been normalized to unity. The fluorescence yields tend to alter the profiles of the relative intensities greatly by accentuating the lower charge states and reducing the amount of the higher charge states. For the 24-MeV O^{+8} case the KL^4 peak contains only 10% of the total x-ray intensity but it has the largest relative ionization cross section of 35%. If the fluorescence yields of Bhalla, *et al.*[10] are used, the relative ionization cross sections will change for the higher ionization states. Figure 6 shows the relative cross sections for the 21-MeV N^{+7} case obtained using ω_{KL^n} by Stolterfoht *et al.*[32] (lower) and by Bhalla *et al.*[10] (upper). It is seen that the KL^6 values in the upper figure have a much larger intensity than in the lower figure. This is because the calculations of Bhalla *et al.*[10] do not take into account the closed Auger channel of the $(1s2p^2)^2P$ and ^4P states.

To obtain $P_L(0)$ a least-squares fit to a binomial distribution is performed on the data in Table VI. The probability for ionizing the $2s$ and $2p$ subshell is assumed to be equal. Hopkins *et al.* have shown that treating the probability for ionization of the $2s$ and $2p$ subshells as being unequal changes $P_L(0)$ very little for most physically plausible conditions.[45] $\sigma_{KL^7+KL^8}$ has been fit with the sum of σ_{KL^7} and σ_{KL^8}. This is because the only way to detect σ_{KL^8} is for the neon ion to capture an electron and observe its cascade. The results of the fits are given in Table VI. Several sets of data and their fits are shown in Fig. 7. Also given in Table VI is $\chi^2/(n-1)$, $n-1$ being the number of degrees of freedom, the number of observed peaks minus one, since only $P_L(0)$ is varied in the fitting procedure. It is seen that $\chi^2/(n-1)$ ranges from zero to ten for all spectra except for the F^{+9} spectra. As seen from Fig. 7 the KL^5 peak contains more intensity than can be predicted from a binomial distribution. The other data are seen to have a reasonably good fit.

The values of $P_L(0)$ range from 0.287 for 18-

TABLE VI. Relative ionization cross section σ_{KL^n} and probability for ionization at zero impact parameter $P_L(0)$. V_L is the relative velocity of the projectile (see Sec. VI).

Beam (energy)	V_L	Relative ionization cross sections σ_{KL^0}	σ_{KL^1}	σ_{KL^2}	σ_{KL^3}	σ_{KL^4}	σ_{KL^5}	σ_{KL^6}	$\sigma_{KL^7+KL^8}$	$P_L(0)$	$\frac{\chi^2}{n-1}$
C^{+3} (18 MeV)	6.68	0.052	0.185	0.304	0.286	0.121	0.047	0.005		0.287	3.10
C^{+4} (18 MeV)	6.68		0.148	0.264	0.373	0.144	0.061	0.010		0.314	1.53
C^{+5} (18 MeV)	6.68		0.133	0.253	0.346	0.171	0.082	0.014		0.333	1.99
C^{+6} (18 MeV)	6.68		0.112	0.213	0.254	0.256	0.118	0.035	0.011	0.396	0.80
N^{+4} (21 MeV)	6.68		0.091	0.254	0.385	0.177	0.074	0.014	0.004	0.340	2.59
N^{+6} (21 MeV)	6.68			0.168	0.352	0.267	0.176	0.033	0.005	0.384	9.18
N^{+7} (21 MeV)	6.68			0.097	0.220	0.301	0.265	0.086	0.032	0.485	2.05
N^{+7} (25.5 MeV)	7.36		0.076	0.176	0.331	0.235	0.107	0.059	0.016	0.420	4.66
O^{+4} (24 MeV)	6.68		0.068	0.240	0.292	0.284	0.092	0.024		0.365	6.33
O^{+5} (24 MeV)	6.68			0.198	0.377	0.255	0.144	0.025		0.379	5.59
O^{+5} (30 MeV)	7.47		0.134	0.259	0.285	0.201	0.090	0.025	0.006	0.364	0.38
O^{+6} (24 MeV)	6.68			0.188	0.344	0.269	0.149	0.042	0.008	0.394	1.04
O^{+6} (35 MeV)[a]	8.07	0.031	0.106	0.228	0.332	0.187	0.096	0.017	0.003	0.351	2.96
O^{+7} (24 MeV)	6.68				0.319	0.351	0.213	0.095	0.022	0.451	0.72
O^{+7} (30 MeV)	7.47		0.083	0.203	0.264	0.258	0.127	0.056	0.011	0.413	1.33
O^{+7} (35 MeV)[a]	8.07		0.076	0.193	0.345	0.224	0.131	0.027	0.004	0.384	6.06
O^{+8} (24 MeV)	6.68					0.354	0.325	0.214	0.107	0.565	1.04
O^{+8} (30 MeV)	7.47					0.372	0.408	0.155	0.065	0.514	7.11
O^{+8} (35 MeV)[a]	8.07			0.116	0.263	0.299	0.199	0.093	0.030	0.483	0.64
F^{+9} (28.5 MeV)	6.68					0.123	0.533	0.073	0.172	0.626	42.14
F^{+9} (35.6 MeV)	7.47					0.137	0.555	0.206	0.102	0.566	40.85
Cl^{+7} (40 MeV)[b]	5.83					0.308	0.350	0.255	0.088	0.570	0.94
Cl^{+11} (40 MeV)[b]	5.83						0.396	0.372	0.232	0.647	0.02
Cl^{+13} (40 MeV)[b]	5.83						0.418	0.271	0.310	0.676	10.51
Ar^{+6} (80 MeV)[c]	7.72				0.225	0.406	0.235	0.091	0.042	0.464	7.39
Ar^{+14} (80 MeV)[c]	7.72					0.198	0.334	0.241	0.227	0.670	2.99

[a] From Ref. 6.
[b] From Ref. 7.
[c] From Ref. 8.

MeV C^{+3} to 0.676 for 40-MeV Cl^{+13}. $P_L(0)$ for the data taken at $V_L = 6.68$ (1.5 MeV/amu) is plotted in Fig. 8 versus the ionic charge of the projectile. The trend previously noted from examination of the x-ray spectra is again seen in the data.[46] This is that projectiles having the same ionic charge produce similar amounts of multiple ionization. This is especially true when a K-shell electron is added to the projectile. The spectra do not show as great of a change in multiple ionization when an L-shell electron is added to the projectile. Also plotted in Fig. 8 is the curve of the prediction of the BEA theory. Values of $P_L(0)$ for these cases are predicted to be from 3.0 to 6.0. This is unphysical since the probability cannot exceed one. The data are seen to be approximately an order of magnitude below the BEA predictions and the data do not show as great an increase as the Z^2 rise predicted by Coulomb ionization theories. In Fig. 9 the energy dependence of O^{+q} is shown. Also given is the energy dependence of the BEA theory. The data although an order of magnitude lower are seen to fall off less than the BEA theory. This is expected since the BEA theory predicts a $1/E$ dependence for high-energy projectiles while Bethe-Born theories predict a correct $\ln E/E$ dependence which is more slowly decreasing.[47]

The relative x-ray intensities R_{KL^n} given in Table II can be used in conjunction with the fluorescence yields ω_{KL^n} given in Table IV to obtain an average fluorescence yield $\bar{\omega}$. Using the formula[5] $\bar{\omega}^{-1} = \sum_n R_{KL^n}/\omega_{KL^n}$, $\bar{\omega}$ for the different collision cases are derived and given in Table VII. The chlorine and argon values are not included because the high-energy excitations are non-negligible in these cases.[7,8] It is seen that $\bar{\omega}$ ranges from 0.027 for 18-MeV C^{+3} to 0.162 for 2.85-MeV F^{+9}. These values are from about 1.7 to 10 times the normal fluorescence yield of 0.016. If the x-ray data are not corrected for this effect, an enormously large charge-state effect would be observed in the low-resolution data. An improved estimate of $\bar{\omega}$ for the cases of large excitation may be obtained by using the binomial fit to the data. In some cases, as for O^{+8}, the lower satellite intensities are not

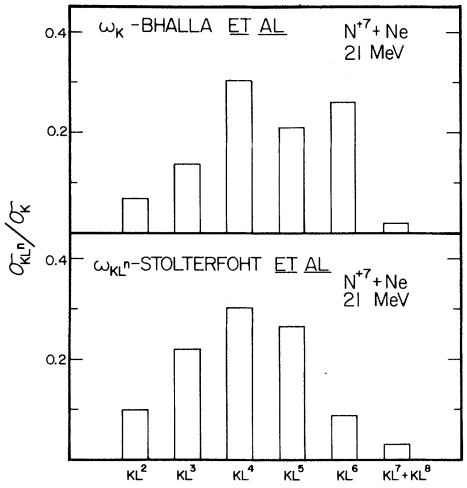

FIG. 6. Relative multiple-ionization cross sections for 21-MeV N^{+7}+Ne. The top figure shows values derived using the fluorescence yields of Bhalla *et al.*[10] The bottom figure shows values derived using semiempirical fluorescence yields. Note the jagged profile of the top figure.

observed because of their small fluorescence yields. They make significant contributions to the Auger yield and thus to $\bar{\omega}$. To account for their effect the fit to the relative ionization cross sections may be used to obtain estimates of their relative x-ray intensities. From these estimates a $\bar{\omega}$ may be derived as before. For 24-MeV O^{+8} a $\bar{\omega}$ from the fit is 0.123 compared to $\bar{\omega}=0.153$ as derived from the data itself. For the cases pro-

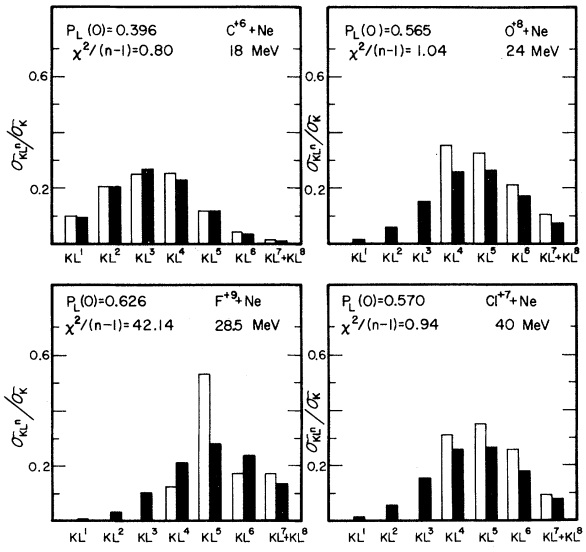

FIG. 7. Relative multiple ionization cross sections and their fits to a binomial distribution. The measured cross sections are given by the light bars. The fits are given by the dark bars. Note the large discrepancy for the 28.5-MeV F^{+9}+Ne case.

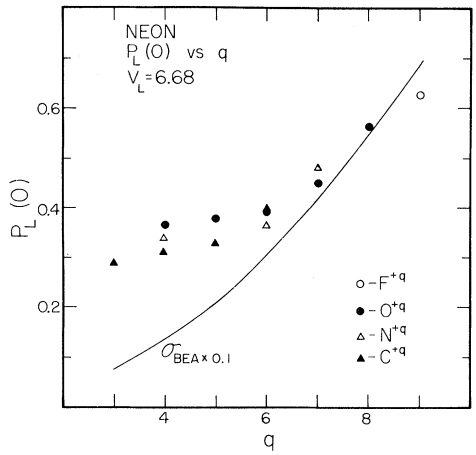

FIG. 8. $P_L(0)$ as a function of ionic charge for projectiles having a relative velocity of $V_L=6.68$ (1.5 MeV/amu). The solid curve is the prediction of the BEA theory which contains a Z^2 dependence. The data rise less than Z^2.

ducing less multiple ionization, such as carbon and nitrogen, the procedure does not give much change in $\bar{\omega}$.

VIII. CONCLUSIONS

The relative multiple ionization cross sections fit a binomial distribution reasonably well. The data do not provide good fits if they are not corrected for the KL^5 and KL^6 overlap or if the fluorescence yields of Bhalla *et al.*[10] are used. These fluorescence yields neglect the closed Auger channel of the $(1s2p^2)^2P$ and ^4P states. In deriving the semiempirical fluorescence yields a binomial distribution is assumed.[32] The two

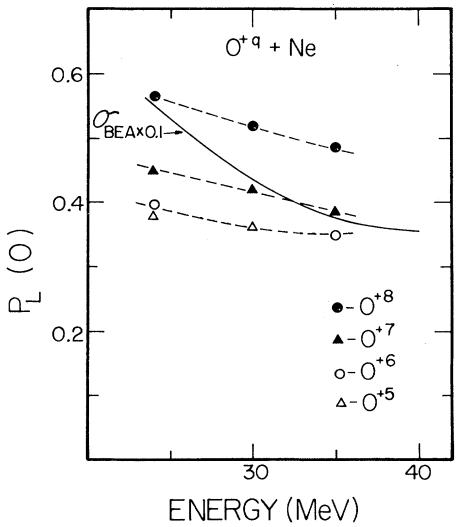

FIG. 9. Energy dependence of O^{+8}+Ne. The solid curve is the prediction of the BEA which falls off faster than the data.

TABLE VII. Average fluorescence yield, $\bar{\omega}$, for C, N, O, and F for various energies and charge states.

Beam	Energy (MeV)	$\bar{\omega}$ Charge state 3	4	5	6	7	8	9
C	18	0.027	0.030	0.032	0.047	•••	•••	•••
N	21	•••	0.034	•••	0.046	0.078	•••	•••
	25.5	•••	•••	•••	•••	0.056	•••	•••
	24	•••	0.039	0.041	0.050	0.078	0.153	•••
O	30	•••	•••	0.039	•••	0.055	0.110	•••
	35	•••	•••	•••	0.035	0.041	0.078	•••
F	28.5	•••	•••	•••	•••	•••	•••	0.162
	35.6	•••	•••	•••	•••	•••	•••	0.151

cases for which the fluorescence yields are derived have differing amounts of multiple ionization but still give consistent sets of values. Also the fluorescence yields give multiple ionization cross sections which fit a binomial distribution over a wide range of values of $P_L(0)$. Thus the fluorescence yields and the data are at least self consistent in regard to the binomial distribution.

The notable exceptions in the data are the F^{+9} cases. The data have much larger KL^5 peaks than are predicted by the binomial distribution. These spectra would be most sensitive to the KL^5-KL^6 correction because most of the ionization is contained in the two peaks. A small error in the amount of correction could distort the multiple ionization values greatly. The chlorine induced spectra and the Ar^{+14} induced spectrum also contain large amounts of multiple ionization but have reasonable fits to a binomial distribution. Another possible explanation for the difference is that another ionization mechanism is present for the F^{+9} case. This is in the near-symmetric collision region so that some vacancy-promotion mechanism may be preferentially exciting in the KL^5 ionization state. Or, a multiplet state with a high fluorescence yield may be preferentially excited so that the statistical excitation assumption is no longer valid.

ACKNOWLEDGMENT

The authors wish to thank Forrest Hopkins in assisting with some of the setup and early data acquisition.

*Work supported in part by the U. S. Energy Research and Development Administration under Contract No. AT(11-1)-2130.

†Work done in partial fulfillment of Ph.D. degree requirements at Kansas State University.

[1]L. M. Winters, J. R. Macdonald, M. D. Brown, T. Chiao, L. D. Ellsworth, and E. W. Pettus, Phys. Rev. A 8, 1835 (1973).

[2]J. R. Mowat, I. A. Sellin, P. M. Griffin, D. J. Pegg, and R. S. Peterson, Phys. Rev. A 9, 644 (1974).

[3]E. Merzbacher and H. W. Lewis, *Encyclopedia of Physics*, edited by S. Flügge (Springer-Verlag, Berlin, 1958), Vol. 34, p. 166.

[4]J. D. Garcia, Phys. Rev. A 1, 1402 (1970).

[5]R. L. Kauffman, F. Hopkins, C. W. Woods, and P. Richard, Phys. Rev. Lett. 31, 621 (1973).

[6]D. L. Matthews, B. M. Johnson, and C. F. Moore, Phys. Rev. A 10, 451 (1974).

[7]M. D. Brown, J. R. Macdonald, P. Richard, J. R. Mowat, and I. A. Sellin, Phys. Rev. A 9, 1470 (1974); P. Richard, R. L. Kauffman, S. J. Czuchlewski, C. W. Woods, and K. A. Jamison (unpublished).

[8]J. R. Mowat, R. Laubert, I. A. Sellin, R. L. Kauffman, M. D. Brown, J. R. Macdonald, and P. Richard, Phys. Rev. A 10, 1446 (1974).

[9]D. Burch, W. B. Engalls, J. S. Risley, and R. Heffner, Phys. Rev. Lett. 29, 1719 (1972).

[10]C. P. Bhalla, N. O. Folland, and M. A. Hein, Phys. Rev. A 8, 649 (1973).

[11]J. M. Hansteen and O. P. Mosebekk, Phys. Rev. Lett. 29, 1361 (1972).

[12]J. H. McGuire and P. Richard, Phys. Rev. A 8, 1374 (1973).

[13]J. L. Jones, K. W. Paschen, and J. B. Nicholson, Appl. Opt. 2, 955 (1963).

[14]Siemens Corporation, Karlsruhe, Germany.

[15]J. D. Garcia and J. E. Mack, J. Opt. Soc. Am. 55, 654 (1965).

[16]N. J. Peacock, R. J. Speer, and M. G. Hobby, J. Phys. B 2, 798 (1969).

[17]R. L. Blake (private communication).

[18]J. R. Macdonald, S. M. Ferguson, T. Chiao, L. D. Ellsworth, and S. A. Savoy, Phys. Rev. A 5, 1188 (1972).

[19]F. Hopkins, R. L. Kauffman, C. W. Woods, and P. Richard, Phys. Rev. A 9, 2413 (1974).

[20]D. L. Matthews (private communication). Used computer code given in Ref. 24.
[21]R. L. Kauffman, C. W. Woods, K. A. Jamison, and P. Richard, Phys. Lett. 50A, 117 (1974).
[22]R. L. Kauffman, C. W. Woods, F. F. Hopkins, D. O. Elliott, K. A. Jamison, and P. Richard, J. Phys. B 6, 2197 (1973).
[23]C. L. Cocke, B. Curnutte, and R. Randall, Phys. Rev. A 9, 1823 (1974).
[24]C. F. Fischer, Comp. Phys. Commun. 4, 107 (1972).
[25]H. P. Summers, Astrophys. J. 179, L45 (1973).
[26]P. Richard, R. L. Kauffman, C. W. Woods, and K. A. Jamison, Phys. Rev. Lett. 30, 888 (1973); P. Richard, R. L. Kauffman, F. Hopkins, C. W. Woods, and K. A. Jamison, Phys. Rev. A 8, 2187 (1973).
[27]D. J. Pegg, I. A. Sellin, R. Peterson, J. R. Mowat, W. W. Smith, M. D. Brown, and J. R. Macdonald, Phys. Rev. A 8, 1350 (1973).
[28]C. P. Bhalla, Phys. Lett. 46A, 185 (1973).
[29]E. U. Condon and G. H. Shortley, *The Theory of Atomic Spectra* (Cambridge U. P., Cambridge, England, 1959), p. 371.
[30]R. Marrus and R. W. Schmieder, Phys. Rev. A 5, 1160 (1972).
[31]C. P. Bhalla, D. L. Matthews, and C. F. Moore, Phys. Lett. 46A, 336 (1974).
[32]N. Stolterfoht, D. Schneider, P. Richard, and R. L. Kauffman, Phys. Rev. Lett. 33, 1418 (1974).
[33]D. L. Matthews, B. M. Johnson, L. E. Smith, J. J. Mackey, and C. F. Moore, Phys. Lett. 48A, 93 (1974).
[34]G. W. F. Drake, Astrophys. J. 158, 1199 (1969).
[35]G. W. F. Drake, Phys. Rev. A 3, 908 (1971).
[36]G. W. F. Drake and A. Dalgarno, Astrophys. J. 157, 459 (1969).
[37]C. Bhalla, Physica Fennica, 9, Suppl. S1, 435 (1974).
[38]M. H. Chen and B. Craseman, Physica Fennica, 9 Suppl. S1, 250 (1974).
[39]J. D. Garcia, R. J. Fortner, and T. M. Kavanagh, Rev. Mod. Phys. 45, 111 (1973).
[40]J. S. Briggs and J. Macek, J. Phys. B 5, 579 (1972).
[41]U. Fano and W. Lichten, Phys. Rev. Lett. 14, 627 (1965); M. Barat and W. Lichten, Phys. Rev. A 6, 211 (1972).
[42]W. E. Meyerhoff, Phys. Rev. A 10, 1005 (1974).
[43]J. Bang and J. M. Hansteen, Kgl. Danske Videnskab Selskab, Mat.-Fys. Medd. 31, No. 13 (1959); J. M. Hansteen and O. P. Mosebekk, Nucl. Phys. A 201, 541 (1973).
[44]R. L. Kauffman, J. H. McGuire, P. Richard, and C. F. Moore, Phys. Rev. A 8, 1233 (1973).
[45]F. Hopkins, D. O. Elliott, C. P. Bhalla, and P. Richard, Phys. Rev. A 8, 2952 (1973).
[46]R. L. Kauffman, C. W. Woods, K. A. Jamison, and P. Richard, J. Phys. B 7, L335 (1974).
[47]J. D. Garcia, E. Gerjuoy, and J. E. Walker, Phys. Rev. 165, 66 (1968).